Advances in Aircraft and Spacecraft Science, *Vol. 4, No. 6 (2017) 679-699*
DOI: https://doi.org/10.12989/aas.2017.4.6.679

Impact of composite patch on the J-integral in adhesive layer for repaired aluminum plate

D. Ait Kaci*[1], K. Madani[1a], M. Mokhtari[1], X. Feaugas[2] and S. Touzain[2]

[1]Laboratoire Mécanique Physique des Matériaux (LMPM), Department of Mechanical Engineering, University of SidiBel Abbes, Sidi Bel Abbes 22000, Algeria
[2]LaSIE, UMR7356, Laboratoire des Sciences de l'Ingénieur pour l'Environnement, Université La Rochelle, Av. Michel Crépeau, 17042 La Rochelle, France

(Received May 26, 2017, Revised July 12, 2017, Accepted July 31, 2017)

Abstract. The aim of this study is to perform a finite element analysis of the Von Mises stresses distribution in the adhesive layer and of the J-Integral for a damaged plate repaired by a composite patch. Firstly, we study the effect of the fiber orientation, especially the position of the layers that have orientation angle different of 0° from the first layer which is in all cases of our study oriented at (0°) on the J-Integral. Secondly, we evaluate the effects of the mechanical properties of the patch and the use of a hybrid patch on the reduction of stresses distribution and J-Integral. The results show clearly that the stacking sequence for the composite patch must be selected to absorb optimally the stresses from the damaged area and to position the various layers of the composite under the first layer whose fibers orientation will remain in all cases equal to 0°. The use of a hybrid composite reduces significantly the J-Integral and the stresses in both damaged plate and the adhesive layer.

Keywords: plane-strain; numerical simulation; composites; damage analysis; delamination; fibre composite multilayer plates; modelling

1. Introduction

Composite materials in advanced engineering structures have gained great popularity over the past decades because of their high strength/weight ratios and high damping capacity (Içten *et al.* 2002). The use of composite materials to repair damaged structures has evolved rapidly in different fields. Compared to mechanically fastened joints, adhesively bonded joints have many advantages such as load distribution over larger area due to absence of holes, no damage to composite material due to hole machining, no increment of weight due to the fasteners weight and no stress concentrations due to the presence of holes (Elhannani *et al.* 2016, Benchiha *et al.* 2015, 2016). However, stress concentrations always occur at the edge of adhesive layer in adhesively bonded joints (Erdogan *et al.* 1971, Da Costa Mattos *et al.* 2012). Therefore, adhesively bonded joints are more preferable to mechanical joints in joining composite materials (Içten *et al.* 2002).

*Corresponding author, E-mail: aitkaci07@yahoo.fr
[a]Ph.D., E-mail: koumad10@yahoo.fr

http://www.techno-press.org/?journal=aas&subpage=7 ISSN: 2287-528X (Print), 2287-5271 (Online)

Adhesive bonding dates back to the dawn of aviation and far beyond to ancient times (Hart-Smith 1987). While early aircraft were made of wood, the majority of twentieth century planes used primarily metal structures with mechanical fastening as joining mechanism. However, current emphasis has been on the use of composite materials with bonding as primary means for joining components. A detailed study of adhesive bonded metallic structures is reported in the Primary Adhesively Bonded Structure Technology (PABST) Program (Içten *et al.* 2002). In the last couple of decades, bonding of fiber reinforced polymer composite materials has become the focus of research.

Adhesively bonded repairs using boron/epoxy and graphite/epoxy patches have also some drawbacks. One of the main disadvantages of these patch materials results from their relatively low thermal expansion coefficient compared to the metallic substrate (Erdogan *et al.* 1971). Bonding composite patches on the damaged areas is a local repair method frequently used in industry (Thrall 1977, 1979). To reconstitute the mechanical performance of a repaired structure as close as possible to that of the original one, the patch has to be carefully designed. The success of the repair depends on the coherence between the base structure material and the patch, the adhesive used, the surface treatment, as well as the skills of repair operators (Grabovac and Whittaker 2009, Campilho *et al.* 2005). Botelho (2009) has studied the fatigue behavior of repaired aramid fiber/epoxy composites. His work presents the structural repair influence on tensile and fatigue properties of a typical aramid fiber/epoxy composite used in the aerospace industry. According to this work, the aramid/epoxy composites with and without repair present a high tensile strength values. Therefore, the fatigue results show that the repaired aramid/epoxy composite presented low fatigue resistance in low and high cycle when compared with non-repaired composite. The repair of cracks in aluminum structures by composite patch has been studied to a great extent. Tenchev (2008) conducted an experimental and numerical study of the static and fatigue performance of a composite adhesive repair on 5HS/RTM6 composite intact coupons and coupons incorporating adhesively-bonded (FM300-2) stepped flush joints. The results show that the adhesive joint, which is widely used in repairs, significantly reduces the static strength as well as the fatigue life of the composite. Both, the static and the fatigue failure of the ‘repaired’ coupons occur at the adhesive joint and involve crack initiation and propagation. There have also been many studies involving the effect that stiffening members have on crack growth. Moreira (2015) has presented in his study the characterization of composite bonded single-strap repairs under fatigue loading, High cycle fatigue behaviour of single-strap repairs of carbon–epoxy laminates was analyzed experimentally and numerically. Static and fatigue tests were performed under three-point bending loading. The numerical approach is based on a mixed-mode I and II cohesive zone modelling accounting for quasi-static and fatigue degradation through a unique damage parameter. It was verified that numerical fatigue life prediction is in the range of the fatigue life observed experimentally.

Double-sided or symmetric patching is the strongest configuration when applying a composite patch. This has been shown as an effective means of lowering the Stress Intensity Factor (SIF) and in turn increasing the fatigue life (Gong *et al.* 2007, Costa *et al.* 2012). Symmetric patching has been shown the most effective way to provide a more even distribution of stress across the thickness of the plate. For the same configuration, a study showed that a double-sided patch has twice the fatigue life of a single-sided patch (Belhouari *et al*. 2004).

The analysis of adhesively bonded joints requires a reliable and efficient tool to obtain stresses and strains distributions. For this purpose, different techniques (analytical modeling and numerical solution) have been used in the past to predict the strength and stress distributions of adhesively bonded composite joints. After many years of study, various repair techniques have been successfully applied. Among them, adhesively bonded structural repair has gained more use than mechanically fastened structural repair for the reason that fiber reinforced composites are essentially bonded in nature. Therefore, in recent years, several experimental (Tsai and Shen 2004, Klung and Sun 1998) and numerical studies (Charalambides *et al.* 1998, Bartholomeusz *et al.* 1999) have been conducted to investigate the influence of different repair parameters on the stress distribution, ultimate strength, and stress intensity factor of the bonded repaired structures. Liu *et al.* (2007) conducted experimental tests and a 3-D progressive damage model was developed. They found a good agreement between the experimental and numerical results. Using their model, the effects of several repair parameters on failure initiation strength, ultimate strength and failure mechanism of the repaired structures were investigated. Sabelkin *et al.* (2007), have studied by a combined experimental–analytical approach several parameters/factors related to mechanical and fatigue behaviors of a cracked 7075-T6 aluminum panel repaired with one-sided adhesively bonded composite patch. Hosseini-Toudeshky *et al.* (2009) investigated by the numerical and experimental fatigue crack growth the behaviour of centrally cracked aluminum panels in mode-I loading condition repaired with single-side composite patches. They have shown that the crack growths non-uniformly from its initial location through the thickness of a single-side repaired panel. There is a good agreement between the propagated crack-front shapes obtained from finite element analysis with those obtained from the experiments for various repaired panels with different patch thicknesses (Naveen Rastogi *et al.* 1883, Charalambides *et al.* 1998). The finite element method (FEM) can be used with a great accuracy to evaluate stress intensity factors and other fracture parameters at the crack tip. The Finite element analysis of composite reinforcement by Mitchell *et al*. (Gong *et al.* 2007) appears to be the first thorough attempt towards an analytical understanding of this class of problems. Later, the finite element method was used by several other authors, among them Jones and Callinan (1979), Daghyani (2003), Ting *et al.* (1999), Mitchel *et al.* (1975), Madani *et al.* (2009), Turaga and Ripudaman (1999), Ayatollahi and Hashemi (2007).

Numerical studies were performed by Hosseini-Toudeshky and Mohammadi (Turaga and Ripudaman 1999) to evaluate the thermal residual stress effects on fatigue crack growth of single-side repaired panels bonded with various composite materials in mode-I loading condition. It was shown, that these repairs provide an efficient method for restoring the ultimate load capability of the structure (Turaga and Ripudaman 1999). The analysis of the effects of the geometrical properties of the composite on the repair performance has got great interest in the literature. A good way to design a patch repair is to maximize the safety-cost ratio by finding the optimal patch shape (Ayatollahi 2007, Hosseini-Toudeshky and Mohammadi 2009). Brighenti *et al*. 2006, Breitzman *et al.* 2009) used the genetic algorithm to optimize the patch shape. By adopting the optimal shape patch, the stress-intensity factor can be reduced to about 50% with respect to that related to a simple shape (square or rectangular) patch. There are many geometric, material and loading parameters affecting the effectiveness of the composite patch repair. Some of the previous studies examined these effects. For example, patch dimensions including patch thickness was studied. (Hosseini-Toudeshky and Mohammadi 2009). The layer orientation of fibrous composite was studied by Ayatollahi (2007) and Ouinas *et al*. (2009).

However, many of these studies did not take into account the effect of both fiber orientation and use of a hybrid composite patch to repair the damaged panels. In the present study, a three-dimensional non-linear finite element code is established to analyze the effects of fiber orientation angle, stacking laminates and use of hybrid composites on both the stress distributions and j-integral of the damaged plate repaired by patch subjected to tensile loading.

2. Finite element model and description of material properties

Let us consider a thin elastic aluminum 2024-T3 plate having dimensions: height, *H*, equal to 250 mm, width, *w*, equal to 125 mm, thickness, *e*, equal to 2 mm. An initial edge crack perpendicular to the loading direction having a length equal to 8 mm is assumed to exist in the plate.

Such a plate is repaired by a rectangular patch and is subjected to an imposed displacement, u, equal to 0.5 mm.

The composite patch is bonded to the cracked plate to strengthen and reduce the stress from the damaged area through the adhesive (Fig. 1). The dimensions of the patch are length H_r =50 mm, width w_r=25 mm and thickness e_r=1 mm.

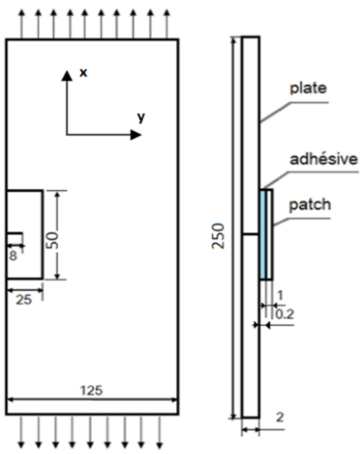

Fig. 1 Geometrical sizes of the repaired plate

Tensile tests performed on 2024-T3 aluminum plate and adhesive ADEKIT A140 have allowed us to have the characteristic curves shown in Fig. 2 (Madani *et al.* 2010).

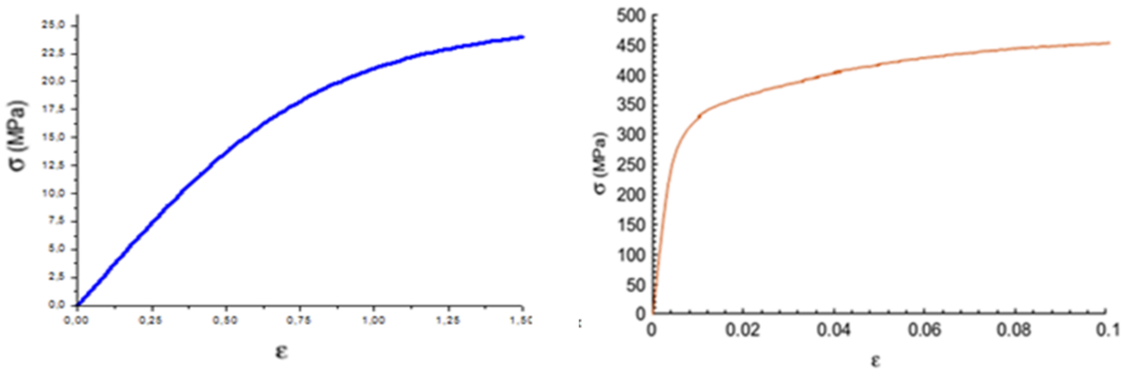

(a) adhesive Adekit A140 (b) aluminum plate

Fig. 2 Tensile stress-strain curve (Madani *et al.* 2010)

From these two curves, we can determine the mechanical properties of the two materials as shown in Table 1.

Table 1 Mechanical properties of aluminum 2024-T3 and adhesive Adekit A140

Material	E (Gpa)	G (Gpa)	*v*
Adekit A140	2.690	0.99	0.3
Aluminum 2024T3	69	36.92	0.3

The analysis was carried out for two composite laminates namely, carbon epoxy (Qing *et al.* 2006) and aramid epoxy (Kilic *et al.* 2006). The properties of the materials used in this study are listed in Table 2.

Table 2 Mechanical properties of composite laminates

Material	E1 (Gpa)	E2 (Gpa)	E3 (Gpa)	G12 (Gpa)	G13 (Gpa)	G23 (Gpa)	*v*12	*v*13	*v*23
Carbon-epoxy	109.000	8.819	8.819	4.315	4.31	3.200	0.342	0.342	0.38
Aramid-epoxy	76	5.5	5.5	2.3	2.3	2.3	0.34	0.34	0.34

These two types of composites were selected to repair the cracked plate and to examine the effect of both changing the thickness of the composite layers and using a hybrid composite aramid/carbon on both the value of the J-Integral and the stress distribution.

Four stacking sequences (Table 3) and three different geometries of the patch (Fig. 3) are considered in this study to investigate their effects on the J-Integral. The angles of the layer orientations layers are measured from the longitudinal direction (see Fig. 1).

Table 3 Different stacking sequences used in the composite

1 - $(0/-45/45/90)_S$	3 - $(0/-45/90/45)_S$
2 - $(0/45/-45/90)_S$	4 - $(0/45/90/-45)_S$

The different configurations of the patch proposed to repair the damaged plate are shown in Fig. 3. First, we used a patch with the same thickness of all layers but different orientations (Fig. 1(a)). Secondly, we modified the value of the thickness of each layer as shown in Figs. 3(b) and 3(c).

The thickness of the layers changes with different patch configurations:

For the patch configuration n°1 of the laminate, the thickness of all layers is identical of each layer is equal to 0.125 mm (Fig. 3(a)).

For the model patch configuration n°2, the thicknesses of the various layers of the laminate are not identical; the layer which is located on the outer of the laminate has a minimum thickness value, the thickness of the layers increases towards the middle of the patch (Fig. 3(b)). Similarly,

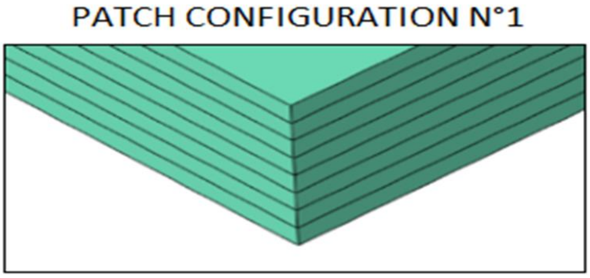

(a) Patch configuration n°1: The thickness of each layer is the same in the composite

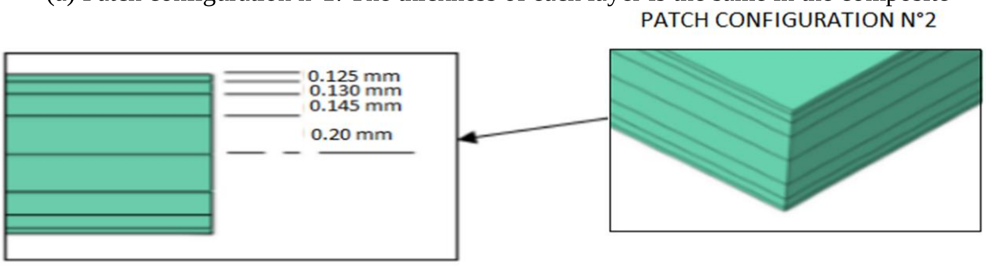

(b) Patch configuration n°2: Minimum value of the thickness for the outer layers and increasing values towards the middle of the composite

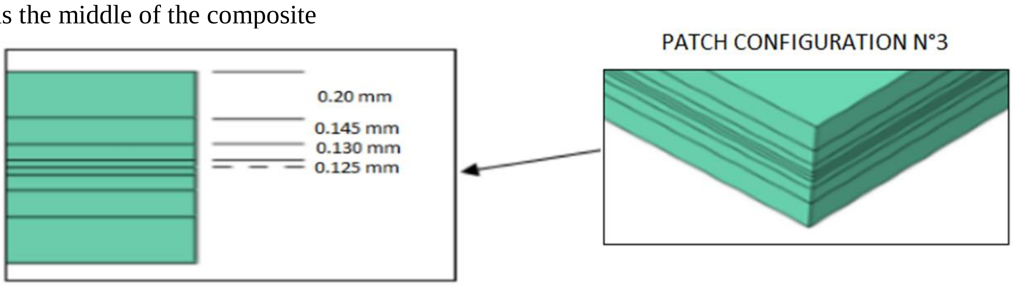

(c) Patch configuration n°3: Maximum value of the thickness for the outer layers and decreasing values towards the middle of the composite

Fig. 3 Representation of the three different patch configurations

for the configuration of the patch configuration n°3, the thicknesses of the different layers are not identical, the thickness of the layer that is on the outer of the laminate has the maximum value and decreases towards the middle of the of the laminate.

In the last part of our study, we modified the mechanical properties of the different layers by choosing a hybrid composite as shown in the following stacking sequences:

$(0_A/-45_A/45_A/90_C)_S$

$(0_A/45_A/-45_C/90_A)_S$

$(0_A/-45_C/90_A/45_A)_S$

$(0_C/45_A/90_A/-45_A)_S$

Where C stays for Carbon fiber and A for Aramid fiber.

We change only the type of fiber nature of two layers, which have the same fiber orientations for the three configurations of patch (see Fig. 3). Hence, we get 8 plies of composite, with 6 of aramid/epoxy and 2 of carbon/epoxy (Fig. 4).

For this choice of hybrid composite, we just tried to change the layers that have the same fiber orientation and this for each stacking sequence.

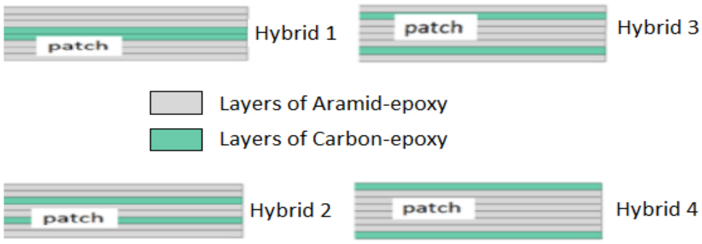

Fig. 4 Different configurations of composite nature (2 layers of Carbon and 6 layers of Aramid fibers)

3. Finite element modeling

Finite element analysis of the repaired plate configurations, shown in Fig. 5, is done using the ABAQUS finite element code.

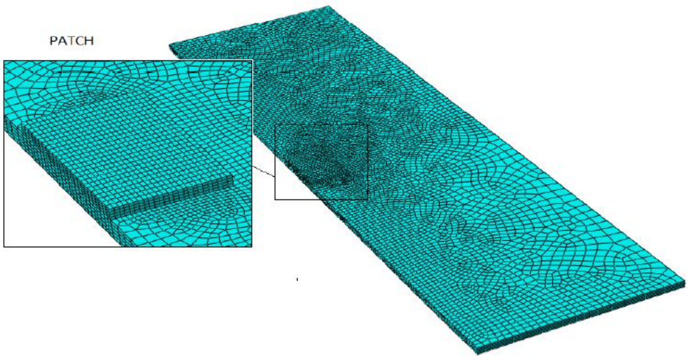

Fig. 5 Mesh details of repaired plate (a) patch zone and (b) crack tip

A layered structure of laminate patch is actually a three-dimensional structure. A three-dimensional finite element model of such a structure involves several degrees of complexity. In order to capture the essential features of the response, we make same simplifying assumptions:
- Each layer is considered as an individual three-dimensional structure which can be connected with adhesive bonds.
- The adhesive layer is homogeneous, elastoplastic and isotropic, it deforms under tensile, shear and peel stresses.
- The adhesive is modeled as a third layer. In the finite element model, the nodes are common between each individual three-dimensional structure to ensure a continuity of deformation and stress.

The technique of the three layers modeling was employed by (Naboulsi 1996). They employed the two-dimensional finite element analysis, composed of three layers, to model the joint. In the technique of the three layers, the adhesive is modeled as a continuous medium replacing the elements of shear spring (non-continuous bodies) commonly used in the existing finite element methods such as the finite element code, Franc2D/L developed by Swenson *et al.* (1998). The advantage of modeling the adhesive as a continuous body is to be able to capture the characteristics of the adhesive, which are required to account for heating effects, a nonlinear behavior of material, progressive damage, etc. The elements used in the modeling of the assemblies are standard quadrilateral 8-node isoparametric.

In this part, the effect of geometrical patch on the fracture behavior of a cracked plate and repaired by patch is studied by the finite element method. The J-integral which quantifies the intensity of the field of stress and strain at the crack tip, and predict the durability of the repair is calculated.

The J-integral is widely accepted as a fracture mechanic parameter for both linear and nonlinear material response. It is related to the energy release associated with crack growth and is a measure of the deformation intensity at a notch or crack tip, especially for nonlinear materials. If the material response is linear, it can be related to the stress intensity factors. Because of the importance of the *J*-integral in the assessment of flaws, its accurate numerical evaluation is essential to the practical application of fracture mechanics in design calculations. Abaqus/Standard provides a procedure for such evaluations of the *J*-integral, based on the virtual crack extension/domain integral methods.

The present study employs the domain-integral approach, as originally developed by Shih *et al*. (1986) to compute the energy release rate along the curved front of the surface crack in three dimensions (see Fig. 6). The local value of the mechanical energy release rate at each point under a static loading condition is given by

$$J(s) = \lim_{\Gamma \to 0} \int \left[W n_1 - \sigma_{ij} \frac{\partial u_i}{\partial X_1} n_j \right] d\Gamma$$

where Γ is a vanishingly small contour in the normal plane to the crack front at s, and n_j is the unit vector normal to the contour Γ, W is the strain energy density, σ_{ij} is the component of the nominal stress tensor, u_i is the displacement vector, and X_i is the local Cartesian coordinate system at the locations on the crack front.

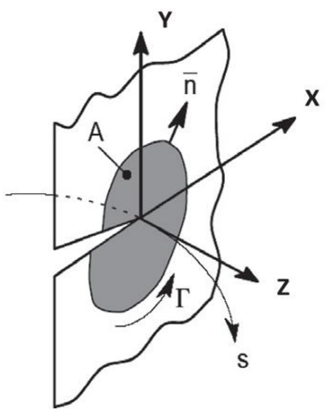

Fig. 6 Contour of the *J*-integral calculation

4. Analysis and results

4.1 Effect of geometrical configurations of the patch on the stress distribution

4.1.1 Von Mises stress distribution in each layer of the composite

To study the effect of different configurations of the patch on the charge transfer from the plate to the patch through the adhesive, we presented, in Fig. 7. the distribution of the equivalent Von Mises stress in the different in layers of the patch and the stresses distribution at the patch/adhesive interface. In this part of the study, the stacking sequence chosen is $[0]_8$.

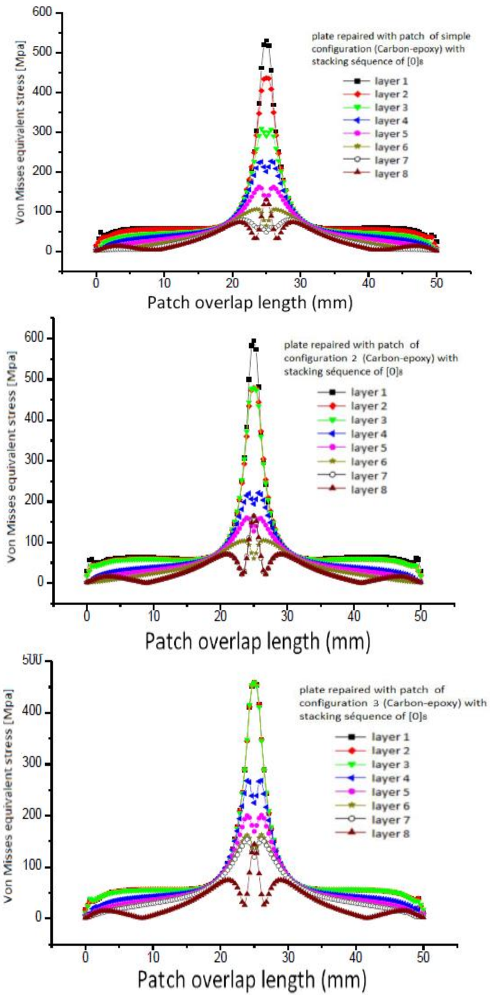

Fig. 7 Comparison of the stress distributions inside the different layers for the three configurations of patch (laminate $[0]_8$)

The first observation is that the stresses distribution in the different plies is identical regardless of the type of changes made to the patch.

The stress is highest in the first layers, which is in contact with the adhesive. Going towards the outside of the patch, the value of the stress decreases.

The stress is concentrated at the crack tip and decreases going towards the free edge of the patch.

Therefore, the various changes to the geometry of the patch do not affect the stress distribution in the patch and the load transfer plate/adhesive/patch.

The maximum stress values are present in the patch with the configuration n°2. The patches with the configuration n°1 and configuration n°2 absorb more stress from the damaged plate than the patch of configuration n°3.

The bending effect due to the eccentricity of the neutral axis caused by the repair by simple patch induces stress at the levels at the edge.

The measurement of the deformation of the repaired structure clearly shows that its value is significantly higher in the case of patch repair of configuration N° 3 (Fig. 8).

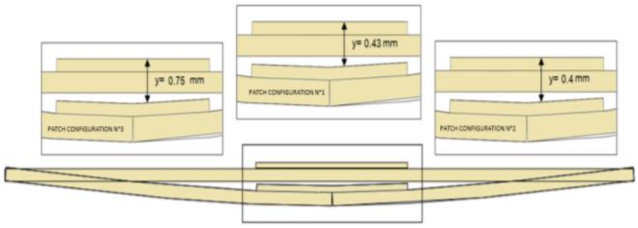

Fig. 8 Bending of the repaired plate according to each patch configuration $[0]_8$

The stress distribution in the adhesive layer presents the maximum values at the edges and crack tip.

The load transfer through the adhesive is very important for the different patch configuration. The patch in configuration n°2 causes high stress in the adhesive layer.

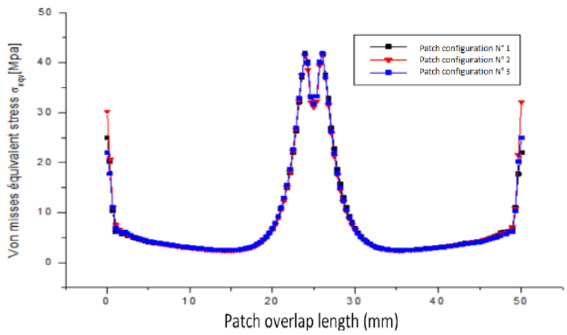

Fig. 9 Comparison of the stress distributions related to the three-geometrical modification of the patch at the interface plate/adhesive (composite Carbon/epoxy with laminate sequence of $[0]_8$)

Similarly, the stress level in the plate shows clearly that the patch with patch in configuration 1 absorbs more stresses from the plate than the two other patches configuration and therefore less stress in the plate (Fig. 10).

4.2 Variation of J-Integral

4.2.1 Effect of the geometrical modifications of the patch on the value of the J-Integral

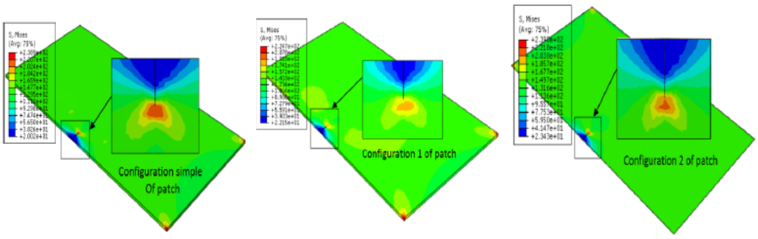

Fig. 10 Stress level in the repaired plate for each patch configuration (stacking sequence chosen $[0]_8$)

To analyze the effect of the different repair patch configurations on the J-Integral value, taking into account the different stacking sequences listed in Table 3. We used carbon/epoxy as the patch material.

The crack length is constant and equal to 8mm; we took only the maximum value of the J-Integral for different parameters considered in this study.

In our study, the different stacking sequences selected have the same fiber orientations except that the location of layers is not the same. The fiber orientation in the first layer is always equal to 0° whatever the stacking sequence.

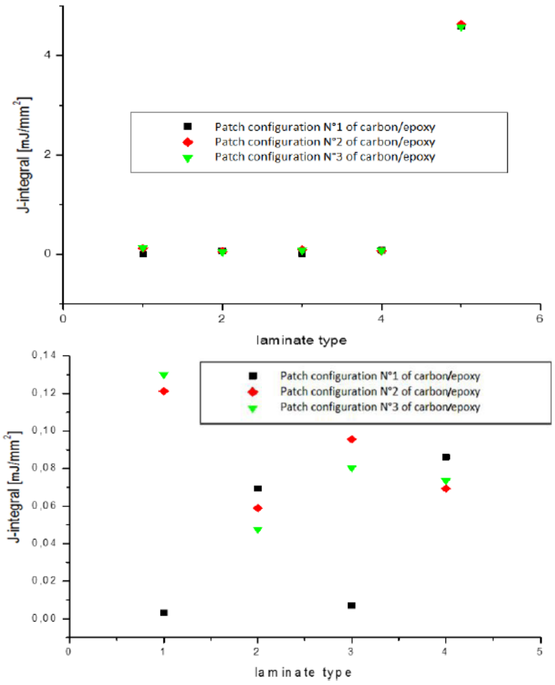

Fig. 11 Variation of the J-Integral according to different stacking sequences for the various configurations of patch (carbon/epoxy)

According to Fig. (11(a)), it's clearly seen that the value of the J-Integral depends strongly on the stacking sequence of the composite patch and especially according to the location of the layers which the fiber orientation is different from 0 °.

The maximum value of the J-Integral is obtained for the case where all the layers are oriented at 0° (unidirectional composite). In this case, the patch is too rigid (high Young's modulus) and therefore, the stresses are more concentrated in the plate leading to a high value of the J-Integral. The value of the J-Integral of the plate repaired by the unidirectional patch is much higher than the other values of J-Integral for a plate repaired by the patch of different configurations, which is why we presented in the Fig. (11(b)) just the values of the J-integral for the 4 other stacking sequences.

In Fig. (11(b)), the value of J-Integral is minimal in the case where the patch has a simple configuration [thickness of the layers is identical] with the stacking sequences of $(0/-45/\ 45/90)_S$ and $(0/-45/90/45)_S$. However, in the case of the stacking sequence of $(0/45/-45/90)_S$, the value of the J-Integral is minimal for a plate repaired by a patch configured according to model 2.

The value of the J-Integral is the lowest in the case where the plate is repaired by a patch whose configuration is type 1 with a stacking sequence of $(0/45/90/-45)_S$.

Whatever the kind of the geometric modification of the patch and the stacking sequence, the value of the J-Integral is still minimal compared to the case of a repaired patch with a stacking sequence of $[0]_8$.

This behavior is almost the same even if we change the nature of the composite, tacking such as material nature of the repaired composite the aramid/epoxy (Fig. 12).

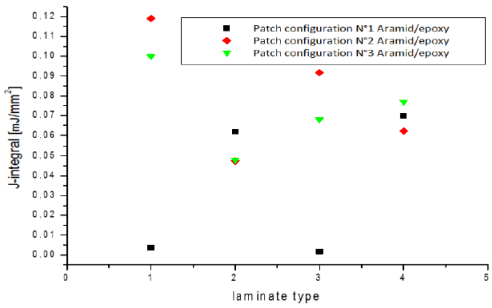

Fig. 12 Variation of the J-Integral according to different stacking sequences for the various configurations of the repair patch (aramid/epoxy)

The load transfer from the damaged plate to the patch goes through the adhesive which is the weak link in the structure. The analysis of the stresses in the adhesive is essential to avoid the breaking of this latter.

Fig. 13 represents the variation of the equivalent Von Mises stress in the adhesive layer according to different stacking sequences for the different geometric configurations of the patch.

As can be noted, the value of the von Mises stress is influenced by the type of configurations of the patch and simultaneously by the stacking sequence. The minimum value of the Von Mises stress is obtained for the case of a plate repaired by patch with layers of the same thickness and (patch simple configuration) with a stacking sequence of the type [0/-45/90/45]s.

For the case of reparation with a patch configured according to model 2, regardless of the stacking sequence, there is always the maximum value of Von Mises stress in the layer of the adhesive.

For the case of reparation with the patch configured according to model 1, the value of the Von Mises stress is the highest for the case where the stacking sequence is $[0/-45/45/90]_S$.

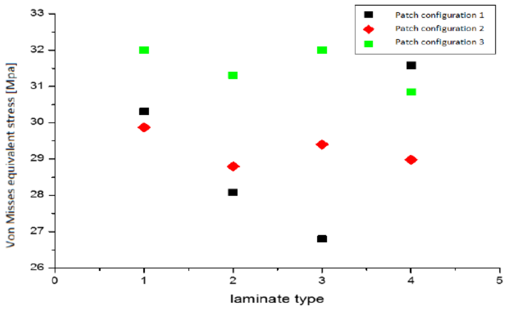

Fig. 13 Variation of the Von Mises stress in the adhesive layer for different patch configurations according to the different stacking sequences

For the repair of a damaged plate by a composite patch with layers of different fibers orientations, it is essential to make the best choice for the position of these layers to avoid the maximum stress in the adhesive layer.

4.2.2 Effect of the use of a hybrid composite

Repair with a hybrid composite material is not very used because this technique is new in the aviation sector. The objective of this section is to analyze by means of the finite elements method the effect on the value of the J-Integral of the use of a hybrid composite patch.

In this section of the paper, we will try to repair the damaged plate by a hybrid composite: in this case, the laminate composite has more aramid than carbon layers.

We know very well that the carbon / epoxy patch absorbs more stresses than the aramid/epoxy patch due to its high mechanical properties. The nature of composite materials plays an important role in the delay of the crack propagation and brings a long service life of the structure. This is why most repair patches are based on carbon, boron and graphite.

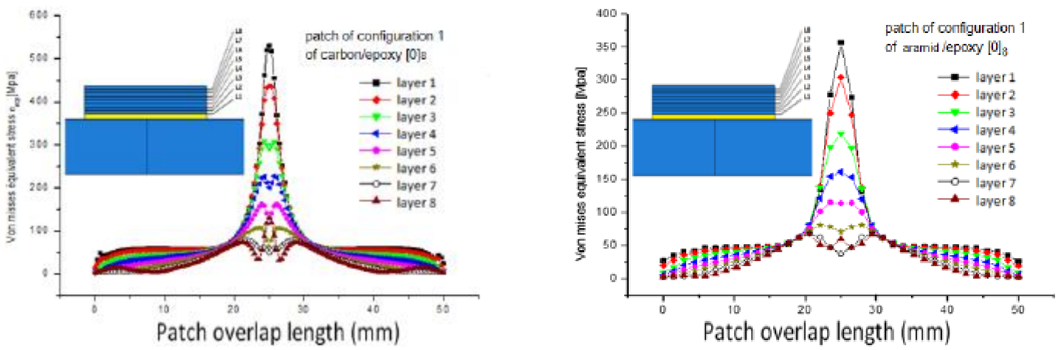

(a) carbon/epoxy (b) aramid/epoxy

Fig. 14 Stress distribution in the different layers of the composite

In Fig. 14, we present the distribution of Von Mises stress in the composite patch for different fiber types (a patch Aramid/epoxy and another carbon/epoxy).

The stress distribution in the various layers of the repaired composite is identical whatever the nature of the fiber material. Except that the patch of carbon/epoxy has higher values compared to the aramid/epoxy patch. These maximum values are caused by a better load transfer from the plate to the patch, so in most cases, the patch repair is chosen too rigid in order to have a better stress transfer (Fig. 14). The aramid/epoxy patch absorbs the stress from the damaged plate but it still lower than those of the carbon patch.

The charge transfer rate from one layer to another is substantially the same regardless of the nature of the fiber.

To see the effect of using a hybrid patch on the reduction of the value of J-integral of the plate and stress in the adhesive layer, we wanted to strengthen the aramid/epoxy composite with layers of carbon/epoxy, so we will have 6 layers of aramid and 2 layers carbon. The position of the two carbon layers in the hybrid composite varies according to the configurations presented in Fig. 15.

For each hybrid composite, the orientation of the two layers of carbon/epoxy varies according to stacking sequences selected from Table 3.

Also, we tried to study for each case of hybrid composite, the influence of the geometric changes of the patch according to models 1, 2, or simple (Fig. 3).

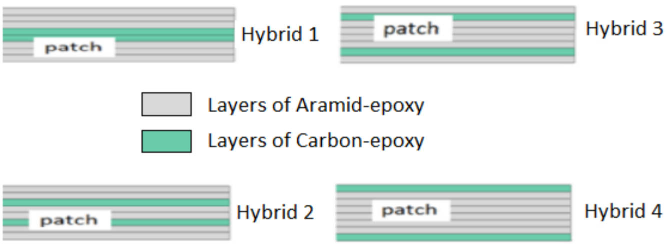

Fig. 15 Different configuration of the hybrid composite

The analysis of the results related to different parameters on the value of the J-integral for the plate repaired by hybrid composite patch is shown in Fig. 16.

The hybrid composite patch reduces greatly the values of J-integral over a patch of aramid/poxy, in the hybrid patch; the position of the two carbon layers plays an important role in reducing the value of the J-integral. Also it is necessary to note, that the fiber orientation of the other layers affects also the value of the J-integral.

The value of the J-integral is minimal in the case of stacking sequences $(0/\text{-}45/45/90)_S$ and $(0/\text{-}45/90/45)_S$ with the hybrid patch configurations respectively (hybrid 1and hybrid 2).

The value of the J-integral is maximal when the two carbon layers are right after the first layer of the composite patch.

However, if the patch has the stacking sequence $(0/45/\text{-}45/90)_S$, it is preferable to use a composite with the second configuration of hybrid with the same thickness for all layers.

Similarly, we try to analyze the value of the J-integral for the two others patch configurations (the thickness of the layers are not the same Fig. 3(b) and (c).

For this two patch models, whatever hybrid or not, the values of the J-integral are slightly higher than for a plate repaired by a simple patch where the thickness of the various layers is identical.

The lower value of the J-integral is noticed for the case where the patch is hybrid and the position of the two carbon layers are in the middle of the composite (hybrid1) with a stacking

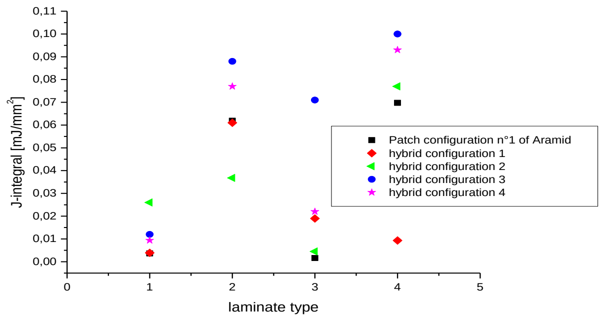

(a)

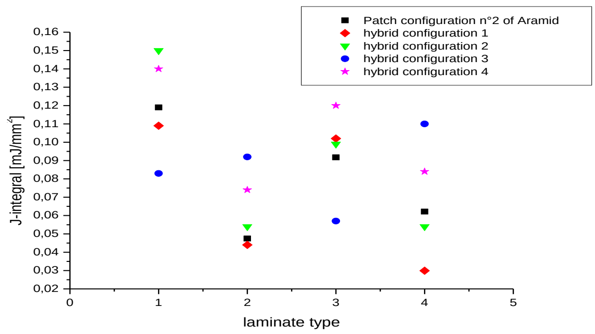

(b)

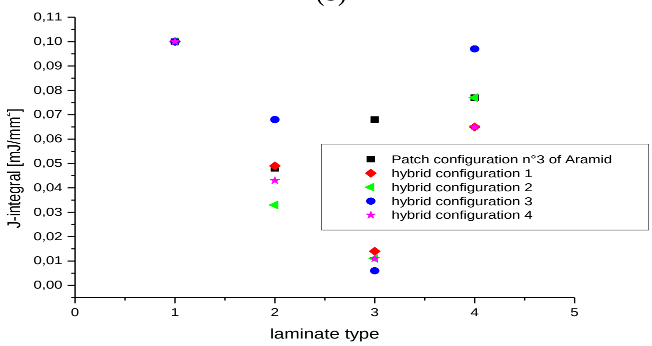

(c)

Fig. 16 Representation of the maximum values of J-integral for the different models of hybrid composite based on different stacking sequences. (a) patch configuration n°1, (b) patch configuration n°2, (c) patch configuration n°3

sequence $(0/45/90/-45)_S$. However, the greatest value is noticed for a hybrid composite 2 and a stacking sequence $(0/-45/45/90)_S$.

For the third configuration of the patch, we clearly see that the value of the integral J varies at the same time with the stacking sequence and the arrangement of the carbon layers with respect to the aramid layers.

If the stacking sequence is of type $(0/-45/45/90)_S$, it is noted that the arrangement of the two carbon layers does not affect the value of the integral J.

The lower value is observed for the stacking sequence $(0/-45\ /90/45)_s$ with hybrid composite type3.

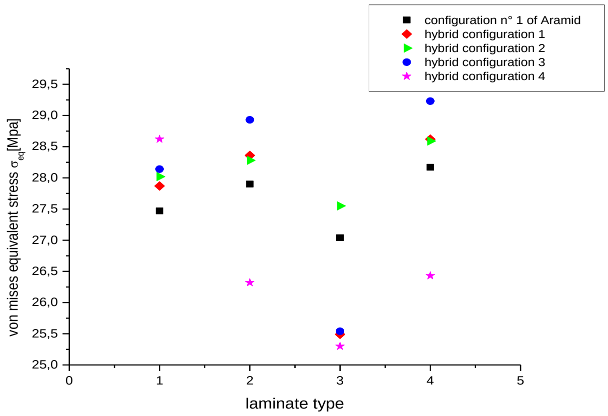

(a)

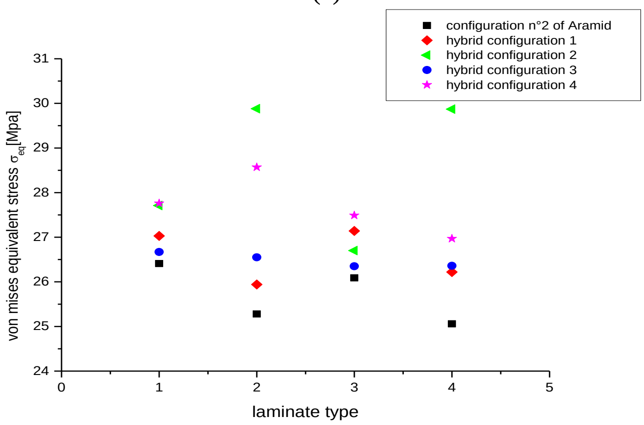

(b)

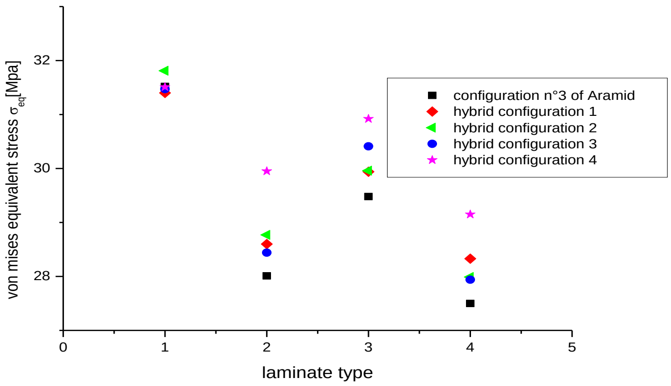

(c)

Fig. 17 Variation of Von Mises stress for the different models of hybrid composite based on different stacking sequences. (a) patch configuration n°1, (b) patch configuration n°2, (c) patch configuration n°3

4.2.3 Distribution of stresses in the adhesive layer

In order to see if the geometric change of the patch, the stacking sequences and the use of hybrid composite have an influence on the value of the equivalent stress in the adhesive layer, the maximum value of the Von Mises stress for the different parameters of the composite patch was represented in Fig. 17.

If the plate is repaired by patch composite with layers thickness is changes according to the configuration 2 (Fig. 3), it is preferable to use a simple patch where the layers are all in Aramid/Epoxy because the hybrid patch gives maximum values in the adhesive layers (Fig. 17(b).

For the patch model with layers thickness changes according to the configuration 3 (Fig. 3), the maximum value of the Von Mises stress is observed for a patch with a stacking sequence (0/-45/45/90)s. Where, whatever the hybrid composite type used, there is always a maximum value of the Von Mises stress. The lower values are noted for the stacking sequences (0/45/-45/90) sand (0/45/90/-45)s with a simple composite patch where all layers are in Aramid/Epoxy (Fig. 17(c)).

To see clearly the charge transfer in the various layers of the hybrid composite, we determine the Von Mises stress distribution in the different layers of the different configuration of the hybrid composite (Fig. 18).

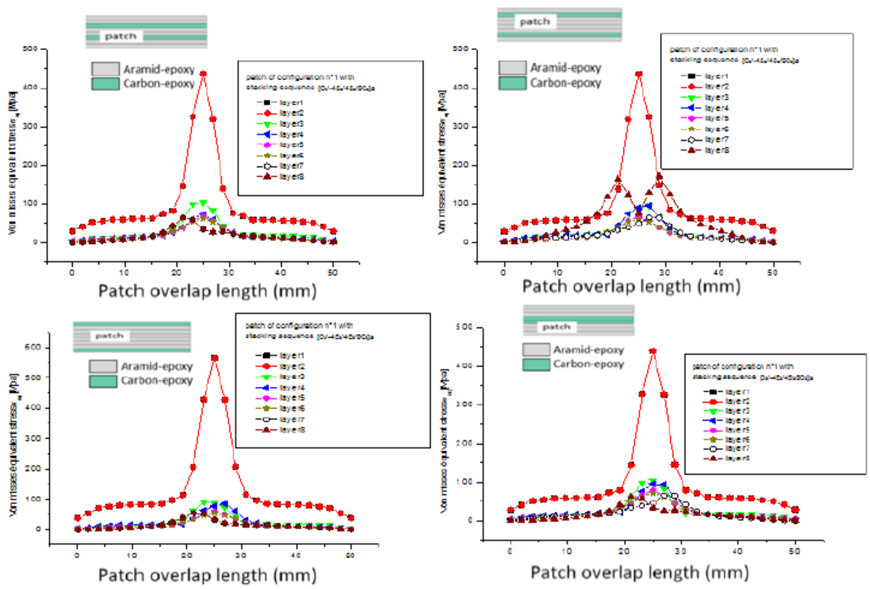

Fig. 18 Distribution of Von Mises stress along the length of the patch in the different layers according to the different types of the hybrid composite ($(0/-45/45/90)_S$) (all layers of the patch have the same thickness)

It is clearly seen, that the stress distribution is the same regardless of the type of hybrid composite, the maximum value in the layer of the patch is still in the layer which is in contact with the adhesive.

The greatest value of the Von Mises stress is reached in the case of composite patch where the carbon layer is in contact with the adhesive since in this position, the carbon layer can better absorb the stresses from the damaged plate.

In order to see the effect of the stacking sequence, we analyze the distribution of Von Mises stress in the different layers of the four types of the hybrid composite patch for the stacking sequence $[0]_8$. The highest values of the stresses are observed when the carbon layer is in direct contact with the adhesive leading to a good load transfer (Fig. 19).

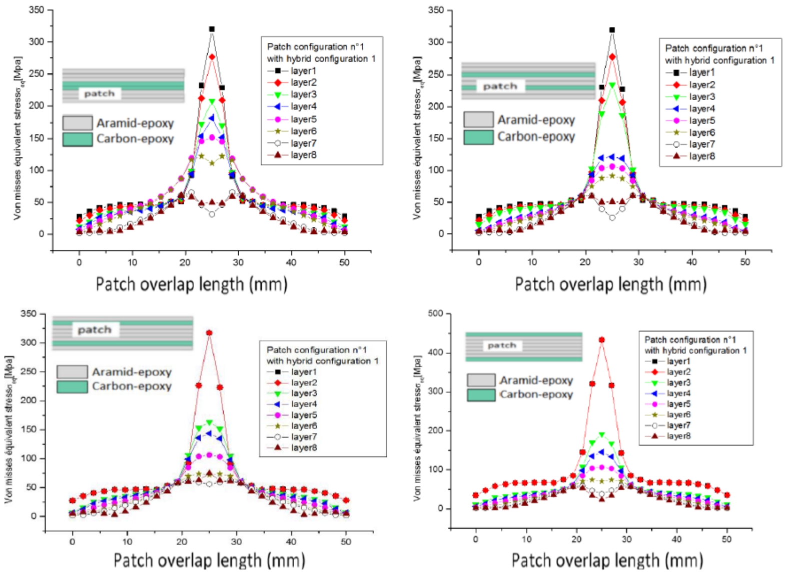

Fig. 19 Distribution of Von Mises stress along the length of the patch in the different layers according to the types of the hybrid composite $[0]_8$ (all layers of the patch have the same thickness)

5. Comparison of results

Patch configuration n°2: Minimum value of the thickness for the outer layers and increasing values towards the middle of the composite.

Patch configuration n°3: Maximum value of the thickness for the outer layers and decreasing values towards the middle of the composite.

Table 4 represents a comparison between the J-Integral values for the different configurations of the patch.

Table 4 Comparison between the J-integral values for the different configurations of the patch. Patch configuration n°1: The thickness of each layer is the same in the composite (a) patch normal

	$(0/45/-45/90)_S$	$(0/45/90/-45)_S$
Patch configuration1	0.07 mj/mm^2	0.085 mj/mm^2
Patch configuration2	-17%	-17%
Patch configuration3	-28%	-11%

(b) Patch hybride configuration1

		$(0/45/-45/90)_S$	$(0/45/90/-45)_S$
	Patch configuration1	0.07 mj/mm^2	0.085 mj/mm^2
Patch configuration1	Patch hybrid configuration1	-5%	+14%
	Patch hybrid configuration2	-48%	-7%
	Patch hybrid configuration3	+25%	+17%
	Patch hybrid configuration4	+12%	+16%

(c) Patch hybride configuration2

		$(0/45/-45/90)_S$	$(0/45/90/-45)_S$
	Patch configuration1	0.07 mj/ mm^2	0.085 mj/ mm^2
Patch configuration2	Patch hybrid configuration1	-35%	-64%
	Patch hybrid configuration2	-25%	-36%
	Patch hybrid configuration3	+34%	+29%
	Patch hybrid configuration4	+7%	-2%

(d) Patch hybride configuration3

		$(0/45/-45/90)_S$	$(0/45/90/-45)_S$
	Patch configuration1	0.07 mj/ mm^2	0.085 mj/mm^2
Patch configuration3	Patch hybrid configuration1	-28%	-24%
	Patch hybrid configuration2	-50%	-8%
	Patch hybrid configuration3	-6%	+15%
	Patch hybrid configuration4	-35%	-24%

For the stacking sequence $(0/-45/45/90)_s$ and $(0/-45/90/45)_s$ the configuration of patch N°1 remains the best compared to the other patch configurations, either the nature of the patch (hybrid or normal).

We have just presented a comparison for the other two stacking sequences $(0/45/-45/90)_s$ and $(0/45/90/-45)_s$. It is noted that for these two sequences of stacks, a significant decrease in the J-Integral value.

This decrease in value depends strongly on the geometry of the patch and the position of the two layers of carbon with respect to the layers of aramid in the hybrid patch.

The better configuration of the patch which brings a better absorption of the stresses in the plate and consequently a reduction of the value of the J-Integral is patch configuration 2 with the laminate sequence $[0_A/45_A/90_A/-45_C]_s$

6. Conclusions

In this study, the effect of geometrical and mechanical parameters of the composite patch and the use of a hybrid patch on the reduction of the value of the J-integral in a repaired plate and the Von Mises stresses distribution in the adhesive layer are numerically investigated. As a result, the following conclusions can be drawn:

• The value of the J-integral is influenced by the stacking sequence.

• 0° orientation is preferable for the first layer of the composite patch since for this orientation charge transfer will be better.

• The carbon/epoxy composite patch absorbs better the stress than the aramid/epoxy patch and therefore a reduction in the value of the J-integral is observed.

• A composite patch possessing fiber orientation 45 90 -45 and 0 is best for a better transfer of charge except that the disposition of these layers with different angles must be optimized to minimize the value of the J-integral and therefore reduce the stresses in the adhesive layer.

• The use of a hybrid composite is essential in the case where the repaired composite has a low rigidity with respect to the damaged plate.

• For the hybrid composite, the arrangement of the carbon layers with respect to the Aramid layers must be optimized in order to have better charge transfer and therefore a minimum value of the integral J.

References

ABAQUS/CAE (2015), *Ver 6.14 User's Manual*, Hibbitt, Karlsson & Sorensen, Inc.

Ayatollahi, M.R. and Hashemi, R. (2007), "Computation of stress intensity factors (KI, KII) and T-stress for cracks reinforced by composite patching", *Compos. Struct.*, **78**(4), 602-609.

Bartholomeusz, R.A., Baker, A.A., Chester, R.J. and Searl, A. (1999), "Bonded joints with through-thickness adhesive stresses-reinforcing the F/A-18 Y470.5 bulkhead", *J. Adhes.*, **19**(2-3), 173-180.

Belhouari, M., Bouiadjra, B.B., Megueni, A. and Kaddouri, K. (2004), "Comparison of double and single bonded repairs to symmetric composite structures: a numerical analysis", *Compos. Struct.*, **65**(1), 47-53.

Benchiha, A. and Madani, K. (2015), "Influence of the presence of defects on the stresses shear distribution in the adhesive layer for the single-lap bonded joint", *Struct. Eng. Mech.*, **53**(5), 1017-1030.

Benchiha, A., Madani, K., Touzain, S., Feaugas, X. and Ratwani, M. (2016), "Numerical analysis of the influence of the presence of disbond region in adhesive layer on the stress intensity factors (SIF) and crack opening displacement (COD) in plates repaired with a composite patch", *Steel Compos. Struct.*, **20**(4), 951-962.

Botelho, E.C. (2009), "Fatigue behavior study on repaired aramid fiber/epoxy composites", *J. Aerosp., Technol. Manage. V*, **1**(2), 217-221.

Breitzman, T.D., Iarve, E.V., Cook, B.M., Schoeppner, G.A. and Lipton, R.P. (2009), "Optimization of a composite scarf repair patch under tensile loading", *Compos. Part A: Appl. Sci. Manufact.*, **40**(12), 1921-1930.

Brighenti, R., Carpinteri, A. and Vantadori, S. (2006), "A genetic algorithm applied to optimization of patch repair for cracked plates", *Comput. Meth. Appl. Mech. Eng.*, **196**(1), 466-475.

Campilho, R.D.S.G., Moura, M.F.S.F. and Domingues, J.J.M.S. (2005), "Modeling single and double-lap repairs on composites materials", *Compos. Sci. Technol.*, **65**(13), 1948-1958.

Charalambides, M.N., Hardouin, R., Kinloch, A.J. and Matthews, F.L. (1998), "Adhesively-bonded repairs to fiber-composite materials", *I. Exper. Compos. A*, **29**(11), 1371-1381.

Charalambides, M.N., Kinloch, A.J. and Matthews, F.L. (1998), "Adhesively-bonded repairs to fiber-composite materials II, finite element modeling", *Compos. A*, **29**(11), 1383-1396.

Costa Mattos, H.S., Monteiro, A.H. and Palazzetti, R. (2012), "Failure analysis of adhesively bonded joints in composite materials", *J. Mater. Des.*, **33**, 242-247.

Costa, T.R.F. Serrano, A.M., Atman, A.P.F., Loguercio, A.D. and Reis, A. (2012), "Durability of composite repair using different surface treatments", *J. Dentist.*, **40**(6), 513-521.

Elhannani, M., Madani, K., Mokhtari, M., Touzain, S., Feaugas, X. and Cohendoz, S. (2016), "A new analytical approach for optimization design of adhesively bonded single-lap joint", *Struct. Eng. Mech.*, **59**(2), 313-326.

Erdogan, F. and Ratwani, M. (1971), "Stress distribution in bonded joints", *J. Compos. Mater.*, **5**(3), 378-393.

Gong, X.J., Cheng, P., Rousseau, J. and Aivazzadeh, S. (2007), "Effect of local stresses on static strength and fatigue life of patched composite panels", *Proceedings of the 16th International Conference on Composite Materials*, Kyoto, Japan.

Gong, X.J.P., Cheng, R.J. and Aivazzadeh, S. (2007), "Effect of local stresses on static strength and fatigue life of patched composite panels", *Proceedings of the 16th International Conference on Composite Materials*, Kyoto, Japan.

Grabovac, I. and Whittaker, D. (2009), "Application of bonded composites in the repair of ships structures-a 15-year service experience", *Compos. Part A*, **40**(9), 1381-1398.

Hart-Smith, L.J. (1987), “Design of adhesively bonded joints, joining fiber-reinforced plastics”, **19**, 271-311.
Hosseini-Toudeshky, H. and Mohammadi, B. (2009), “Thermal residual stresses effects on fatigue crack growth of repaired panels bounded with various composite materials”, *Compos. Struct.*, **89**(2), 216-223.
Hosseini-Toudeshky, H., Mohammadi, B. and Daghyani, H.R. (2003), “Fatigue crack growth rate of adhesively repaired thin aluminum panels in general mixed-mode condition”, *Proceedings of the 11th Annual Conference on Mechanical Engineering*, Mashad, Iran, May.
Içten, B.M. and Karakuzu, R. (2002), *Compos. Sci. Technol.*, **62**, 1259-1271.
Jones, R. and Callinan, R.J. (1979), “Finite element analysis of patched cracks”, *J. Struct. Mech.*, **7**(2), 107-130.
Kilic, B., Madenci, E. and Ambur, D.R. (2006), “Influence of adhesive spew in bonded single-lap joints”, *Eng. Fract. Mech.*, **73**, 1472-1490.
Klung, J.C. and Sun, C.T. (1998), “Large deflection effects of cracked aluminum plates repaired with bonded composite patches”, *Compos. Struct.*, **42**(3), 291-296.
Liu, X. and Wang, G. (2007), “Progressive failure analysis of bonded composite repairs”, *Compos. Struct.*, **81**(3), 331-340.
Madani, K. (2010), “Experimental and numerical study of repair techniques for panels with geometrical discontinuities”, *Comput. Mater. Sci.*, **48**(1), 83-93.
Madani, K., Touzain, S., Feaugas, X., Roy, A. and Cohendoz, S. (2009), “Analyze of the notch effect on the distribution of the stresses in the adhesive layer between two bonded aluminum 2024-T3 plates”, *J. Mater. Technol.*, **97**(5), 315-324.
Mitchel, R.A., Woolley, R.J. and Chwirut, D.J. (1975), “Analysis of composite reinforced cut-outs and cracks”, *AIAA J.*, **13**(6), 744-749.
Moreira, R.D.F., De Moura, M.F.S.F., Figueiredo, M.A.V., Fernandes, R.L.A. and Gonçalves, J.P.M. (2015), “Characterisation of composite bonded single-strap repairs under fatigue loading”, *J. Mech. Sci.*, **103**, 22-29.
Naboulsi, S. and Mall, S. (1996), “Modeling of a cracked metallic structure with bonded composite patch using the three layer technique”, *Compos. Struct.*, **35**(3), 295-308.
Naveen, R., Soni, S.R. and Denney, J.J. (1883), “Analysis of bonded composite patch repaired metallic structures-an overview of aging aircraft”, **AIAA98**, 1578-1588.
Ouinas, D., Hebbar, A., Bachir Bouiadjra, B., Belhouari, M. and Serier, B. (2009), “Numerical analysis of the stress intensity factors for repaired cracks from a notch with bonded composite semicircular patch”, *Compos. B Eng.*, **40**(8), 804-810.
Qing, X.P., Beard, S.J., Kumar, A. and Hannum, R. (2006), “A real-time active smart patch system for monitoring the integrity of bonded repair on an aircraft structure”, *Smart Mater. Struct.*, **15**(3), 66-73.
Sabelkin, V., Mall, S., Hansen, M.A. and Derriso, R.M. (2007), “Investigation into cracked aluminum plate repaired with bonded composite patch”, *Compos. Struct.*, **79**(1), 55-66.
Shih, C.F., Moran, B. and Nakamura, T. (1986), “Energy release rate along a three-dimensional crack front in a thermally stressed body”, *J. Fract.*, **30**, 79-102.
Tenchev, R.T. and Falzon, B.G. (2008), “An experimental and numerical study of the static and fatigue performance of a composite adhesive repair”, *Key Eng. Mater.*, **383**, 10.4028.
Thrall Jr Edward, W. (1977), “Primary adhesively bonded structure technology”, *J. Aircraft*, **14**, 588-594.
Thrall Jr Edward, W. (1979), “PABST program test results”, *Adhes. Age*, **22**, 22-33.
Ting, T., Jones, R., Chiu, W.K., Marshall, I.H. and Greer, J.M. (1999), “Composites repairs to rib stiffened panels”, *Compos. Struct.*, **47**(1), 737-743.
Tsai, G.C. and Shen, S.B. (2004), “Fatigue analysis of cracked thick aluminum plate bonded with composite patches”, *Compos. Struct.*, **64**(1), 79-90.
Turaga, V.R.S. and Ripudaman, S. (1999), “Modeling of patch repairs to a thin cracked sheet”, *Eng. Fract. Mech.*, **62**(2), 267-289.

EC